Journal of Engineering Science and Technology
Vol. 15, No. 1 (2020) 054 - 065

STRESS ANALYSIS OF FUNCTIONALLY GRADED BEAMS DUE TO THERMAL LOADING

CEM BOĞA*, ONUR SELEK

Adana Alparslan Türkeş Science and Technology University,
Faculty of Engineering, Mechanical Engineering, PO box 01250, Adana, Turkey
*Corresponding Author: cboga@atu.edu.tr

Abstract

In this paper, axial stress analysis of a functionally graded beam (FGB) was performed analytically and numerically under thermal loading. In these analyses, three different FGBs were used. Material properties of these FGBs are varied depending on the power law function along the *z* axis while Poisson ratio was assumed to be constant along the *z*-axis. Analytical formulas were given for axial stress analysis along *z* axis. FGBs were analysed numerically using the ANSYS program. Analytical and numerical results of axial stresses were compared and observed to be in consistence with each other. Then, the effect of different FGB types on axial stress was investigated under thermal loading. After analytical and numerical calculations, it was concluded that the FGM type consisting of Ti-6Al-4V/Al_2O_3 metal ceramic pair had the lowest axial stress values. The results are given in graphs.

Keywords: Finite element method, Functionally graded beam, Power function, Stress analysis, Thermal loading.

1. Introduction

Beams are used to transfer and support loads in many areas of the industry such as construction, machine construction, space and aerospace. With the developing technology, the resistance of these beams to mechanical-thermal loads has gained great importance and the functionally graded materials (FGMs) have been a good alternative material for this purpose. FGMs are kind of composite materials consisting of metal and ceramic pairs that can be produced by powder metallurgy method. Metal surface provides the stronger structure to carry the stress and the higher heat resistivity of the ceramic surface prevents heat transfer. There are many studies about FGMs in the literature.

Arbind et al. [1] used a third-order beam theory based on a couple stress theory designed to perform the bending analysis of the FGM beam. They compared the results with the finite element method. Afsar et al. [2] have described an FGM disk consisting of a combination of Al_2O_3-Al material properties throughout the thickness. They developed an analytical formulation for the thermo-elastic analysis of this disc. Afshin et al. [3] have established equations to investigate the transient thermo-elastic analysis of an axisymmetric hollow cylinder made of FGM. They solved this equation by the separation method and compared finite element results with the analytical results.

Almitani [4] has studied buckling characteristics of both nonlinear symmetric power function and sigmoid-law FGBs. Ben-Oumrane et al. [5] have made a formulation based on classical laminate beam theory, deformation theory, high-grade theories to perform the displacement and stress analysis of a sigmoid beam formed from the combination of Al and Al_2O_3. Benyamina et al. [6] performed the thermo-mechanical bending analysis of ceramic-metal FGM beam in their work. This analysis was performed by using refined exponential shear deformation plate theory. They compared the results with literature.

Chakraborty and Gopalakrishnan [7] have developed a new finite element model for wave propagation analysis of the FGM beam exposed to thermal and mechanical loads. Chen et al. [8] used higher-order shear deformation theory to perform thermal vibration analysis of the FGM beam. Cinefra et al. [9] performed thermo-mechanical analysis of FGM shells consisting of metal and ceramic combinations.

Davoodinik and Rahimi [10] formed linear and nonlinear semi-analytical differential equations to perform the mechanical analysis of a flexible tapered functionally graded beam (TFGM). They analysed TFGM numerically with ANSYS program. Ebrahimi and Salari [11] have examined the behavior of FGM nano beam under the thermal loads under the vibration and buckling. El-Megharbel [12] has examined the behavior of the FGM beam under thermal loads. Megharbel has compared the results of this study with the beam of Timoshenko. Elperin and Rudin [13] used the shock method to perform thermal reliability analysis of FGM. They determined the temperature distribution with Laplace-Hankel integral transformations and developed an analytical solution method.

Elperin and Rudin [14], in their other paper they also used thermal shock method to perform thermal stress analysis of FGM that composed of tungsten-carbide (WC) and steel combination. Evran [15] examined the thermal stress analysis of functional graded layered beams using ANSYS finite element program.

He performed layer positions in beams with Taguchi L16 method depending on the orthogonal array design. Evran [16] has investigated bending stress analysis of axially layered FGM beams from Tungsten Carbide (WC) and Aluminum (Al) combination using Taguchi L16 method the ANSYS program. He used Taguchi method for designing the layers of the beams.

Farhatnia et al. [17] have studied thermo-mechanical stress analysis of FGM beam numerically and analytically. Fu et al. [18] have investigated thermal buckling and postbuckling of functionally graded tubes. Fukui and Watanabe [19] made FGM ring casting from Al and SiC materials by centrifugal casting technique. They performed thermal stress analysis on this ring. They compared the results with the curved beam theory.

Golmakaniyoon and Akhlaghi [20] studied time-dependent creep behavior of FGM beam under thermal stress consisting of Al and SiC materials. Kadoli et al. [21] investigated deflection and stress distribution of FGM beams according to the power law. Kondalarao et al. [22] made the analysis of the FGM conical shaft under thermal and mechanical loads using ANSYS. Kapuria et al. [23] produced layered FGM beams with powder metallurgy and spraying method. They found that the thermal response of these beams experimentally and theoretically.

Bhandari and Purohit [24] studied mechanical deformation of FGM plate according to the various boundary conditions with the power law, sigmoid law and exponential law. Sharma et al. [25] studied the thermo-mechanical analysis of FGM square laminated plate under simply supported boundary condition using first order shear deformation theory and ANSYS program. Pandey and Pradyumna [26] used the finite element equation to analyse the FGM beam model consisting of metal and ceramic under thermal shock and defined the material properties according to the power law. Gönczi and Ecsedi [27] have calculated the thermal stresses and radial displacements of the hollow circular FGM disc exposed to thermal and mechanical loads analytically and numerically. Material properties were assumed depend on an exponential function along the radial direction. They compared the numerical results with an analytical solution of the two-point boundary value problem derived.

Nejad et al. [28] have defined the material properties of the thick-walled cylindrical FGM pressure vessel depending on the exponential function. In order to calculate the radial displacements, radial stress and hoop stresses, they presented closed form analytical equations. They compared the analytical results with the finite element results. Allam et al. [29] performed elastic or viscoelastic analysis of rotating FGM discs with variable thickness. Thickness of disk and orthotropic material properties have changed depending on the exponential function. They compared the radial and tangential stresses and displacement values of the solid and annular discs. Chmielewski and Pietrzak [30] presented examples of different FGM combinations for characterization, production and application in industry.

In this study, the axial stresses of the three different FGM beams, which vary according to the power function and under thermal loading, have been determined analytically and numerically. Unlike many studies in the literature, an equation has been found for the inhomogeneity coefficient of the power function in this study. One of the aims of this study is to find the most ideal of FGM beam types working under thermal loads.

2. Formulation of Simple Power Rule

Here, a square cross-section elastic functionally graded material (FGM) beam was considered $h = 0.03$ (m) and $b = 0.03$ (m) with simply supported ends (Fig. 1).

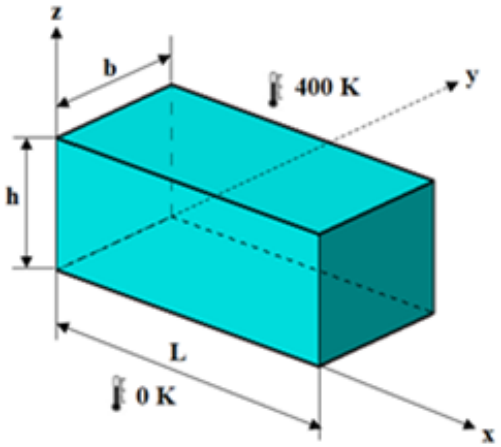

Fig. 1. Isometric view of the functionally graded beam under thermal load.

In this study, the property distribution of FGM material is defined by the power law function along z direction of the beam. The material properties assumed that varying along the z direction as follow:

$$P(z) = P_m \left(\frac{2z+h}{h}\right)^{\beta} \tag{1}$$

If the variation of any property $P(z)$ of the material along the z direction is assumed to obey a simple power rule, the general expression may be written as in Eq. (1). Full metal material at $z = 0$ and full ceramic material at $z = h$ was obtained. The upper surface of the FGM beam is thought to be the ceramic and lower surface metal. While the higher heat resistivity of the ceramic at the upper surface prevents heat transfer, the metal at the lower surface provides the stronger structure to carry the stresses. The boundary conditions (BC's) considered here are:

$$z = 0 \rightarrow P(z) = P_m, \;\; z = h \rightarrow P(z) = P_c \tag{2}$$

If the BC's are applied in Eq. (1), a formula for β can be found as follows:

$$z = h \rightarrow P(z) = P_c \rightarrow P_c = P_m \left(\frac{2h+h}{h}\right)^{\beta}$$

$$P_c = P_m(3)^{\beta} \rightarrow \ln\left(\frac{P_c}{P_m}\right) = \ln(3)^{\beta} \tag{3}$$

In many studies in the literature, inhomogeneity parameter was randomly selected. However, in this study, according to a formula (Eq. 4), which is different from the literature, it was chosen according to the material properties of the metal-ceramic FGM pairs to be examined.

$$\beta = \frac{ln\left(\frac{P_c}{P_m}\right)}{ln\,(3)} \tag{4}$$

Poisson's ratio was assumed constant along the z-axis. $E(z)$, $\alpha(z)$, $k(z)$ and $\rho(z)$ are the modulus of elasticity, the thermal expansion, the thermal conductivity and the density of the beam, respectively, which gives:

$$E(z) = E_m \left(\frac{2z+h}{h}\right)^{\beta_1}, \alpha(z) = \alpha_m \left(\frac{2z+h}{h}\right)^{\beta_2} \quad (5)$$

$$k(z) = k_m \left(\frac{2z+h}{h}\right)^{\beta_3}, \rho(z) = \rho_m \left(\frac{2z+h}{h}\right)^{\beta_4} \quad (6)$$

$$\beta_1 = \frac{\ln\left(\frac{E_c}{E_m}\right)}{\ln(3)}, \beta_2 = \frac{\ln\left(\frac{\alpha_c}{\alpha_m}\right)}{\ln(3)}, \beta_3 = \frac{\ln\left(\frac{k_c}{k_m}\right)}{\ln(3)}, \beta_4 = \frac{\ln\left(\frac{\rho_c}{\rho_m}\right)}{\ln(3)} \quad (7)$$

Figures 2 to 4 show the variation of elasticity modulus, thermal expansion and thermal conductivity of three different types of FGM according to the simple power function respectively.

In Eqs. (5) to (7) subscript *m* refers to metal material and subscript *c* means ceramic material. Material properties of different metals and ceramics for FGM beam are shown in Table 1. Chemical symbol and meaning of ceramics and metals are used as follows in Table 1: Si_3N_4: Silicon Nitride, ZrO_2: Zirconium Oxide, Al_2O_3: Aluminum Oxide, Al: Aluminum, SUS304: Stainless Steel, SUS410: Stainless Steel.

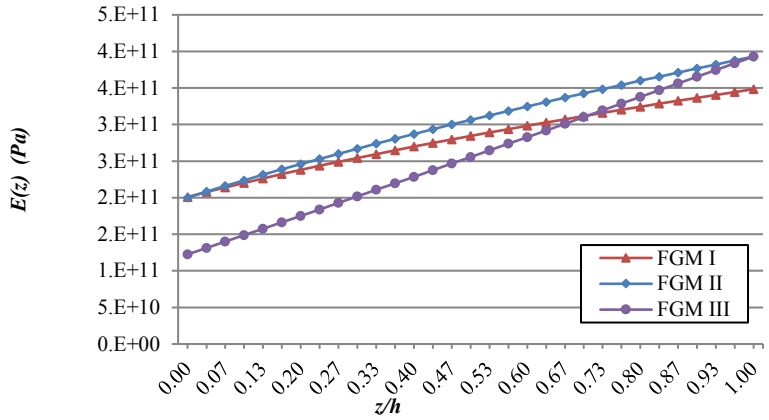

Fig. 2. Variation of elasticity modulus.

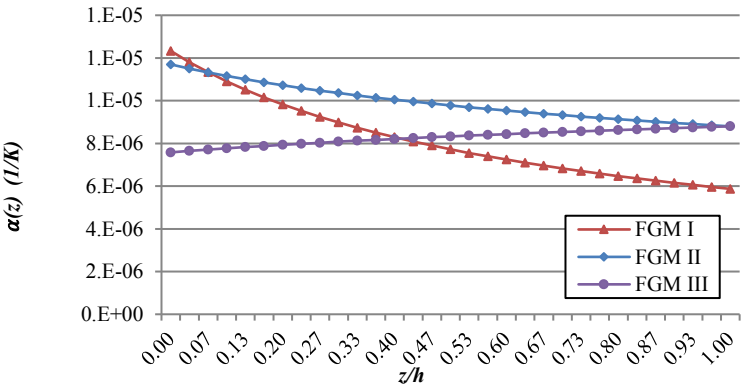

Fig. 3. Variation of thermal expansion.

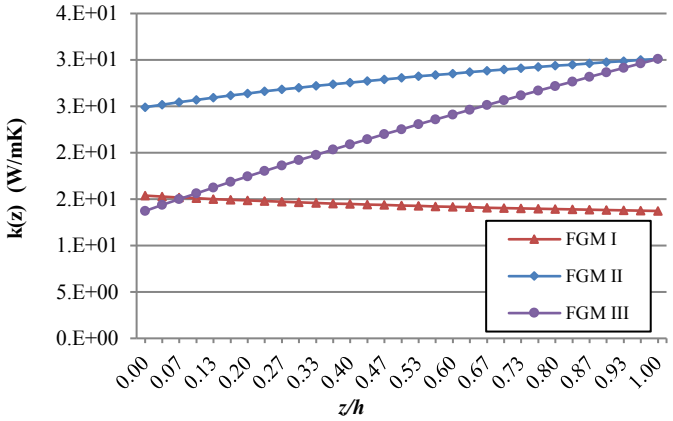

Fig. 4. Variation of thermal conductivity.

Table 1. Material properties of metals and ceramics [31].

Materials (ceramics)	E (GPa)	ρ (kg/m³)	v	k (W/mK)	$\alpha \times 10^{-6}$
Si_3N_4	348.43	3184	0.24	13.723	5.8723
ZrO_2	116.4	3657	0.3	1.78	8.7
Al_2O_3	393	3970	0.3	30.1	8.8
Materials (ceramics)	**E (GPa)**	**ρ (kg/m³)**	**v**	**k (W/mK)**	**$\alpha \times 10^{-6}$**
Ti-6Al-4V	122.557	2370	0.29	13.723	7.579
Al	70	2700	0.3	204	23
SUS304	201.04	7800	0.3262	15.379	12.33
SUS410	200	7750	0.3	24.91	11.7

Along the beam, thickness temperature distribution varies depending on the power function. $T_1 = 0$ (K) and $T_2 = 400$ (K) present temperatures at lower surface and upper surface, respectively (Fig. 5). Equation (8) is for one-dimensional transient heat conduction,

$$\frac{d}{dz}\left[k(z)\frac{dT}{dz}\right] = 0 \tag{8}$$

After solving Eq. (8) the temperature distribution $T(z)$ could be found as follows:

$$T(z) = C_1\left(\frac{2z+h}{h}\right)^{1-\beta_3} + C_2 \tag{9}$$

In Eq. (9), C_1 and C_2 constants can be found after the application of thermal boundary conditions.

$$C_1 = \frac{T_2 - T_1}{(3^{1-\beta_3})-1} \quad , C_2 = \frac{T_1(3^{1-\beta_3}) - T_2}{(3^{1-\beta_3})-1} \tag{10}$$

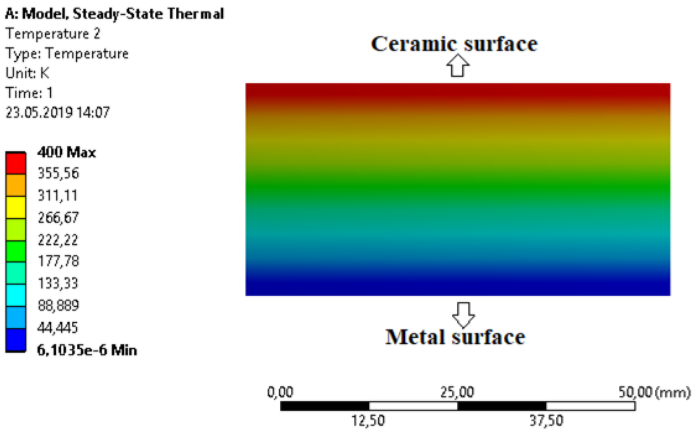

Fig. 5. Temperature distribution along the beam height in ANSYS.

3. Mathematical model of governing equation

The stress-strain relation at the plain strain condition under the thermal loading can be given as follow:

$$\sigma_{xx}(z) = \frac{E(z)}{1-\nu^2}\left[\frac{\partial u_0}{\partial x} - z\frac{\partial^2 w}{\partial x^2} + z\frac{\partial \emptyset_y}{\partial x} - \alpha(z)T(z)(1+\nu)\right] \quad (11)$$

In Eq. (11), u_o is displacement at the $z = 0$, w is the transverse deformation, $\frac{\partial w}{\partial x}$ is rotation of vertical line about y-axis due to the bending and ϕ_y is rotation of vertical line about y-axis due to the shearing deformation. From equilibrium condition, resultant forces in the x-direction are zero and Eq. (12) can be used for the first boundary condition. For second and third boundary conditions, it can be used Eqs. (13) and (14) respectively, which are resultant moments about y-axis under thermal load and simply supported beam. The transverse shear stress is zero due to derivative expressions of u_o, ϕ_y and w. In Eq. (13), I_y can be used $I_y = \frac{bh^3}{12}$ for rectangular and square cross section.

$$\sum F_x = 0 \rightarrow \int_0^h \sigma_{xx}(z)\, b\, dz = 0 \qquad 0 \le x \le L \quad (12)$$

$$\frac{\partial^2 w}{\partial x^2} I_y \int_0^h E(z)\, dz + b\int_0^h z\, E(z)\alpha(z)T(z)\, dz = 0 \quad (13)$$

$$\int_0^h \sigma_{xx}(z)\, z\, b\, dz = 0,\ x = 0; \quad x = L \quad (14)$$

Using metal-ceramic pairs in Table 2, the axial stress expressions could be written according to the parameters given.

Table 2. β values of different metal-ceramic pairs.

Type of FGM	Metal-ceramic pairs	β_1	β_2	β_3
FGM I	SUS304 - Si_3N_4	0.500571	-0.675205	-0.103703
FGM II	SUS410 - Al_2O_3	0.614860	-0.25927	0.172268
FGM III	Ti-6Al-4V - Al_2O_3	1.06064	0.135963	0.714949

Applying the boundary conditions in Eqs. (12) to (14), axial stress expressions analytically may be obtained using Mathematica program for FGM I, FGM II and FGM III as follows in Eqs. (15) to (17) respectively.

$$\sigma_{xx}(z) = 1.26436e^{12}(0.03+2z)^{0.500571}(0.000399023+0.093547z + \frac{0.000251041}{(0.03+2z)^{0.675205}} - 0.0120379(0.03+2z)^{0.428498}) \quad (15)$$

$$\sigma_{xx}(z) = 3.13789e^{9}(0.03+2z)^{0.35559} + 6.40829e^{8}(0.03+2z)^{0.61486} + 2.79246e^{11}z(0.03+2z)^{0.61486} - 5.71706e^{10}(0.03+2z)^{1.18332} \quad (16)$$

$$\sigma_{xx}(z) = 5.53487e^{12}(0.03+2z)^{1.06064}(0.000270755+0.147176z + 0.0171971(0.03+2z)^{0.135963} - 0.0467254(0.03+2z)^{0.421014}) \quad (17)$$

4. Results and Discussion

After the stress values were found analytically, the beam is modelled as FGM in FEM using ANSYS and the results are obtained. Number 1 is the lower metal surface of the beam and number 2 is the upper ceramic surface of the beam in Fig. 6. Numerical analyses for axial stress were modelled according to SOLID279 element type. SOLID279 is a higher order 3-D 20-node solid element that exhibits quadratic thermal behaviour. The element is defined by 20 nodes with a temperature degree of freedom at each node [32]. In meshing, total 54000 elements and 229741 nodes were used for beam analysis. It was compared analytic values with FEM values and it was observed that they were in harmony with each other. And the results were presented graphically in Fig. 7 and % relative error values were given in Table 3.

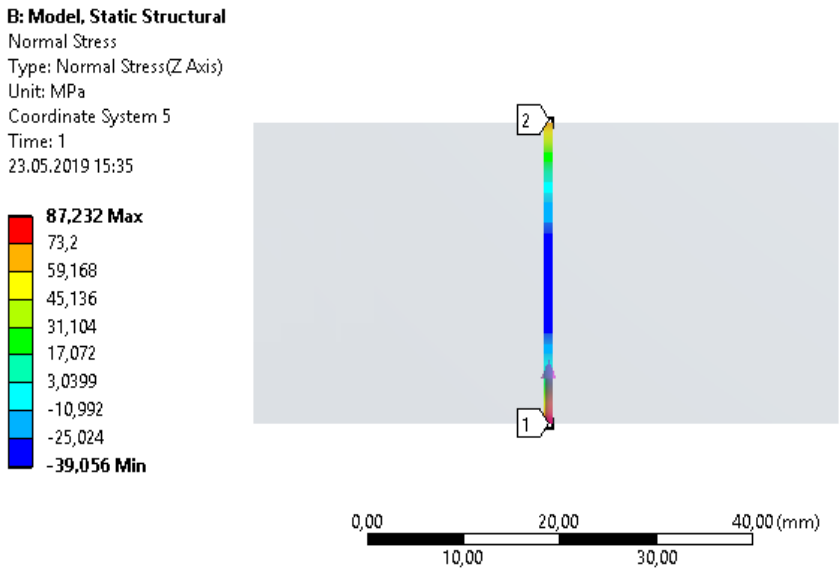

Fig. 6. Finding axial stress values from z =0 to $z = h$ with ANSYS.

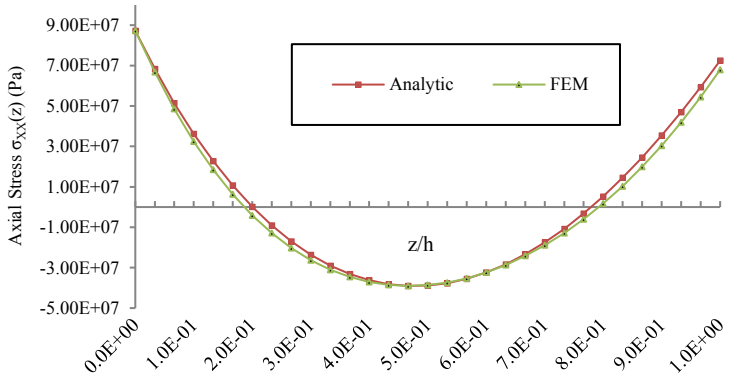

Fig. 7. Comparison of analytic and FEM axial stress results for FGM I.

Table 3. Relative error (%) for analytic and FEM axial stress values of FGM I.

z/h	Analytic	FEM	%Error
0	87208368.41	87232000	-0.027097848
0.1	36307862.03	36293000	0.040933354
0.2	79846.97597	79645	0.252953813
0.3	-23595896.52	-23455000	0.59712299
0.4	-36207543.16	-36079000	0.355017621
0.5	-38858784.23	-38570000	0.743163327
0.6	-32402691.8	-32333000	0.215080282
0.7	-17520077.99	-17431000	0.508433727
0.8	5231719.092	5225200	0.124607074
0.9	35386925.16	35381000	0.016743924
1	72549597.5	72904000	-0.488496859

In Fig. 8, the axial stress values decrease in approaching the midpoints in the *z*-axis direction along the beam thickness for all three FGM type. It is seen that it starts to increase as the midpoints go to the upper surface. As can be seen in Fig. 8 the lowest axial stresses along the thickness of the beam were observed in the FGM III, while the largest stresses were obtained in FGM I. If such a FGM beam is used under thermal loads, low axial stresses are desired for the design. For this reason, FGM III was found to be the most suitable FGM type.

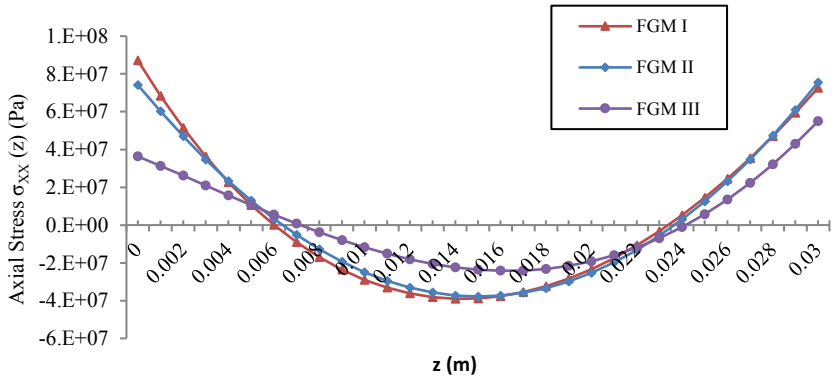

Fig. 8. Comparison of axial stress values for three different FGM.

4. Conclusions

In this study, axial stress analysis of FGM beam under thermal loads was performed analytically and numerically along the z axis. The calculations were made for three different types of FGM. Analytical formulas with respect to z were obtained for the determination of axial stresses. The accuracy of the stress values obtained from these formulas was compared with the numerical method ANSYS. It was shown that axial stress analysis of a FGM beam can be performed quickly and accurately using the FEM with ANSYS program. After the analytical and numerical calculations, the lowest axial stress values, which are the main criteria were obtained from the Ti-6Al-4V/Al_2O_3 metal ceramic pair. In future studies, different FGM pairs can be tested for these loading conditions, and the stress values can be obtained analytically/numerically and the ideal combination can be determined.

Nomenclatures

B	Beam width, mm
E	Modulus of elasticity, Pa
H	Beam thickness, mm
I_y	Inertia moment of rectangular cross section, mm^4
K	Thermal conductivity, W/mK
L	Beam length, mm
N	Poisson's ratio
P_c	Material property of ceramic
P_m	Material property of metal
T	Temperature, K
u_o	Displacement, mm

Greek Symbols

α	Thermal expansion, 1/K
β	Inhomogeneity parameter of material grading function
ρ	Density, kg/m^3
σ_{xx}	Axial stress, Pa

Abbreviations

FEM	Finite Element Method
FGM	Functionally Graded Material
FGB	Functionally Graded Beam

References

1. Arbind, A.; Reddy, J.N.; and Srinivasa, A.R. (2014). Modified couple stress-based third-order theory for nonlinear analysis of functionally graded beams. *Latin American Journal of Solids and Structures,* 11(3), 459-487.
2. Afsar, A.M.; Go, J.; and Song, J.I. (2010). A mathematical analysis of thermoelastic characteristics of a rotating circular disk with an FGM coating at the outer surface. *Advanced Composite Materials***,** 19(3), 269-288.
3. Afshin, A.; Nejad, M.Z.; and Dastani, K. (2017). Transient thermoelastic analysis of FGM rotating thick cylindrical pressure vessels under arbitrary

boundary and initial conditions. *Journal of Computational Applied Mechanics*, 48(1), 15-26.

4. Almitani, K.H. (2018). Buckling behaviors of symmetric and antisymmetric functionally graded beams. *Journal of Applied and Computational Mechanics,* 4(2), 115-124.
5. Ben-Oumrane, S.; Abedlouahed, T.; Ismail, M.; Mohamed, B.B.; Mustapha, M.; and El Abbas, A.B. (2009). A theoretical analysis of flexional bending of Al/Al_2O_3 s-FGM thick beams. *Computational Materials Science,* 44(4), 1344-1350.
6. Benyamina, A.B.; Bouderba, B.; and Saoula, A. (2018). Bending response of composite material plates with specific properties, case of a typical FGM "ceramic/metal" in thermal environments. *Periodica Polytechnica Civil Engineering,* 62(4), 930-938.
7. Chakraborty, A.; and Gopalakrishnan, S. (2003). A spectrally formulated finite element for wave propagation analysis in functionally graded beams. *International Journal of Solids and Structures*, 40(10), 2421-2448.
8. Chen, Y.; Jin, G.; Zhang, C.; Ye, T.; and Xue, Y. (2018). Thermal vibration of FGM beams with general boundary conditions using a higher-order shear deformation theory. *Composites Part B: Engineering,* 153, 376-386.
9. Cinefra, M.; Carrera, E.; Brischetto, S.; and Belouettar, S. (2010). Thermo-mechanical analysis of functionally graded shells. *Journal of Thermal Stresses*, 33(10), 942-963.
10. Davoodinik, A.R.; and Rahimi, G.H. (2011). Large deflection of flexible tapered functionally graded beam. *Acta Mechanica Sinica*, 27(5), 767-777.
11. Ebrahimi, F.; and Salari, E. (2016). Effect of various thermal loadings on buckling and vibrational characteristics of nonlocal temperature-dependent functionally graded nanobeams. *Mechanics of Advanced Materials and Structures*, 23(12), 1379-1397.
12. El-Megharbel, A. (2016). A theoretical analysis of functionally graded beam under thermal loading. *World Journal of Engineering and Technology*, 4(3), 437-449.
13. Elperin, T.; and Rudin, G. (2000). Thermal reliability testing of functionally gradient materials using thermal shock method. *Heat and Mass Transfer,* 36(3), 231-236.
14. Elperin, T.; and Rudin, G. (2002). Thermal stresses in functionally graded materials caused by a laser thermal shock. *Heat and Mass Transfer*, 38(7), 625-630.
15. Evran, S. (2018). Thermal stress analysis of axially layered functionally graded beams using finite element and Taguchi methods. *Eskişehir Technical University Journal of Science and Technology A - Applied Sciences and Engineering,* 19(4), 858-866.
16. Evran, S. (2018). Bending stress analysis of axially layered functionally graded beams. *Ömer Halisdemir Üniversitesi Mühendislik Bilimleri Dergisi*, 7(1), 390-398.
17. Farhatnia, F.; Sharifi, G.-A.; and Rasouli, S. (2009). Numerical and analytical approach of thermo-mechanical stresses in FGM beams. *Proceedings of the World Congress on Engineering.* London, United Kingdom, 6 pages.
18. Fu, Y.; Zhong, J.; Shao, X.; and Chen, Y. (2015). Thermal postbuckling analysis of functionally graded tubes based on a refined beam model. *International Journal of Mechanical Sciences,* 96-97, 58-64.

19. Fukui, Y.; and Watanabe, Y. (1996). Analysis of thermal residual stress in a thick-walled ring of Duralcan-base Al-SiC functionally graded material. *Metallurgical and Materials Transactions A*, 27(12), 4145-4151.
20. Golmakaniyoon, S.; and Akhlaghi, F. (2016). Time-dependent creep behavior of Al-SiC functionally graded beams under in-plane thermal loading. *Computational Materials Science*, 121, 182-190.
21. Kadoli, R.; Akhtar, K.; and Ganesan, N. (2008). Static analysis of functionally graded beams using higher order shear deformation theory. *Applied Mathematical Modelling,* 32(12), 2509-2525.
22. Kondalarao, K.; Hussian, S.R.; and Sreedhar, C. (2016). Thermo-mechanical stress analysis functionally graded tapered shaft system by using ANSYS. *Anveshana's International Journal of Research in Engineering and Applied Sciences*, 1(11), 190-196.
23. Kapuria, S.; Bhattacharyya, M.; and Kumar, A.N. (2008). Theoretical modeling and experimental validation of thermal response of metal-ceramic functionally graded beams. *Journal of Thermal Stresses*, 31(8), 759-787.
24. Bhandari M.; and Purohit, K. (2014). Analysis of functionally graded material plate under transverse load for various boundary conditions. *IOSR Journal of Mechanical and Civil Engineering*, 10(5), 46-55.
25. Sharma, M.; Bhandari, M.; and Purohit, K. (2013). Deflection of functionally gradient material plate under mechanical, thermal and thermomechanical loading. *Global Journal of Researches in Engineering Mechanical & Mechanics,* 13(7), 13-18.
26. Pandey S.; and Pradyumna, S. (2017). Stress analysis of functional graded sandwich beams subjected to thermal shock. *Procedia Engineering*, 173, 837-843.
27. Gönczi D.; and Ecsedi, I. (2015). Thermoelastic analysis of functionally graded hollow circular disc. *Archive of Mechanical Engineering*, 62(1), 5-18.
28. Nejad, M.Z.; Abedi, M.; Lotfian, M.H.; and Ghannad, M. (2016). Exact and numerical elastic analysis for the FGM thick-walled cylindrical pressure vessels with exponentially-varying properties. *Archives of Metallurgy and Materials,* 61(3), 1649-1654.
29. Allam, M.N.M.; Tantawy, R.; Yousof, A.; and Zenkour, A.M. (2017). Elastic and viscoelastic stresses of nonlinear rotating functionally graded solid and annular disks with gradually varying thickness. *Archive of Mechanical Engineering,* 64(4), 423-440.
30. Chmielewski, M.; and Pietrzak, K. (2016). Metal-ceramic functionally graded materials - manufacturing, characterization, application. *Bulletin of the Polish Academy of Sciences Technical Sciences*, 64(1), 151-160.
31. Boğa, C. (2016). *Analytical and numerical axisymmetric elastic stress analyses of stationary/rotating discs made of isotropic/orthotropic functionally graded materials by the transfer matrix method*. Ph.D. Thesis, Çukurova University, Adana, Turkey.
32. Solid 279. 3-D 20-node thermal solid. (2019). Retrieved August 13, 2019, from http://www.mm.bme.hu/~gyebro/files/ans_help_v182/ans_elem/Hlp_E_SOLID279.html.